2D Seismic Analysis of Overpressured Submerged Slopes

A. Stoecklin, A.M. Puzrin

Institute for Geotechnical Engineering, ETH Zürich, Switzerland

1 Introduction

Evidence of past submarine landslides shows that they can reach enormous dimensions of several kilometres in length and width and occur on very mild slopes with gradients of a few degrees. Such underwater mass movements can impose a major hazard on offshore infrastructure and near shore communities due to their tsunami-generating potential (e.g. Tappin et al. 2008). Particularly large and wide spread landslide scars are found in regions where sedimentation rates are high, suggesting that rapid sedimentation plays an important role in their initiation (McAdoo et al. 2000, Urgeles & Camerlenghi 2013).

The stability of submerged slopes is influenced by different processes acting over different time scales, ranging from seconds to thousands of years (Masson et al. 2006). Rapid sedimentation is known as one of the most important long-term landslide pre-conditioning factor. If the deposition of new sediments occurs faster than the consolidation of the underlying soil layers, overpressures (porewater pressures in excess of hydrostatic) develop, leading to a relative weakening of the slope (e.g. Dugan & Sheahan 2012). Recent findings suggest that pre-conditioning by rapid sedimentation can control the occurrence of large submarine landslides with earthquakes acting as the ultimate trigger (Urgeles & Camerlenghi 2013, Stoecklin et al. 2017). Analysing the seismic response of overpressured infinite slope profiles, Stoecklin et al. (2018) showed that the relative weakening by rapid sedimentation can lead to strain localization at a particular depth during earthquake loading.

In this article the effect of pre-conditioning by rapid sedimentation on the expected slope failure mechanisms is investigated. A procedure to model the sediment deposition and subsequent seismic loading of 2D slope geometries is presented and applied to analyse an example case.

2 Methodology

A two-step methodology is developed within the ABAQUS computing environment (Dassault Systèmes Simulia, 2013) to analyse the impact of earthquake events on the stability of overpressured slopes. In the first step the sediment deposition process is modelled, which allows simulating the development of excess pore water pressures as well as the evolution of the density and shear strength of the soil within the sediment layer over time (Section 2.1). In the second step, the impact of earthquakes on the stability of the slope at a specific stage is simulated, using the static stress field and strength-, stiffness and density fields from the sedimentation analysis as initial conditions (Section 2.2). The two-step procedure is described in detail by Stoecklin et al. (2018) for the simplified case of infinite slope conditions. Hence, the subsequently described methodology is focused on the aspects for the analysis of 2D slope geometries, which is required to compute slope failure mechanisms.

2.1 Sedimentation model

The development of overpressures due to sediment deposition occurs on a time-scale of thousands of years and is controlled by fluid flow towards the seafloor. Depending on the deposition rate and the sediments compressibility and permeability, this process can weaken slopes significantly over time. To model this moving boundary value problem, a coupled hydro-mechanical finite element approach is employed, which is described in detail by Stoecklin et al. (2017).

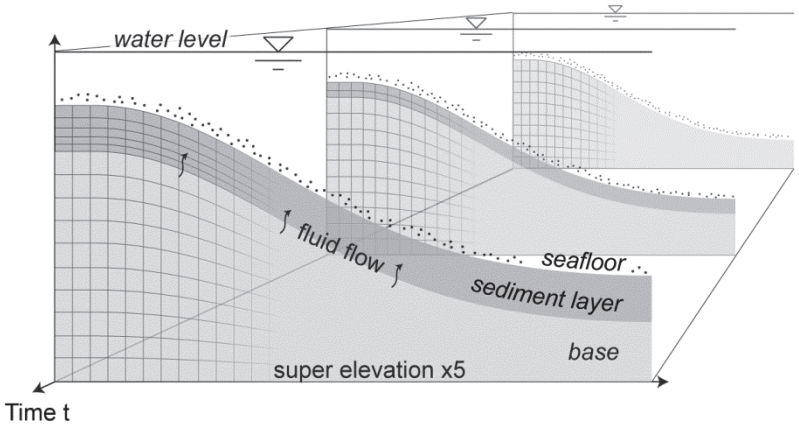

Fig. 1: Illustration of the finite element model for the sedimentation analysis

Elements are stacked over time on a stiff, curved base (Fig. 1). The initial material properties of the newly added elements correspond to the uncompacted sediments near the seafloor. As the sediment layer increases in thickness, the underlying part of the layer undergoes compaction and fluid flow occurs towards the seafloor due to drainage of the pore fluid.

2.2 Seismic model

The impact of seismic events on the stability of submarine slopes is controlled by inertia and the undrained cyclic stress-strain behaviour of the soil. A dynamic total stress finite element approach is employed to model this process, neglecting the fluid flow during the event (Section 2.2.1). To capture the non-linear stress-strain behaviour of the sediments during undrained cyclic loading, a multi-yield-surface kinematic hardening model is used and implemented as user subroutine (Section 2.2.2).

2.2.1 Finite element model

The plane-strain finite element model for the dynamic analysis includes a main model as well as free-field columns at the lateral boundaries. The main model consists of a sediment layer on top of an elastic base (Fig. 2). Infinite elements at the lower boundary provide an absorbing boundary condition during the dynamic analysis, preventing reflection of outgoing waves back into the model while maintaining the reaction forces from static steps (Dassault Systèmes Simulia, 2013). Since the absorbing boundary must be able to move freely to absorb incoming waves, the input time history is transformed and applied at the lower boundary as a shear stress-time history $c_s(t)$ rather than prescribing the acceleration directly (Mejia & Dawson 2006) (Fig. 2). This stress-time history is computed according to equation (1)

$$c_s(t) = 2v_{su}(t)\rho V_s \tag{1}$$

where ρ is the bulk density, V_s the shear wave velocity of the base material and v_{su} is the particle velocity of the upward travelling wave, i.e. half the 'outcrop' motion (Mejia & Dawson 2006).

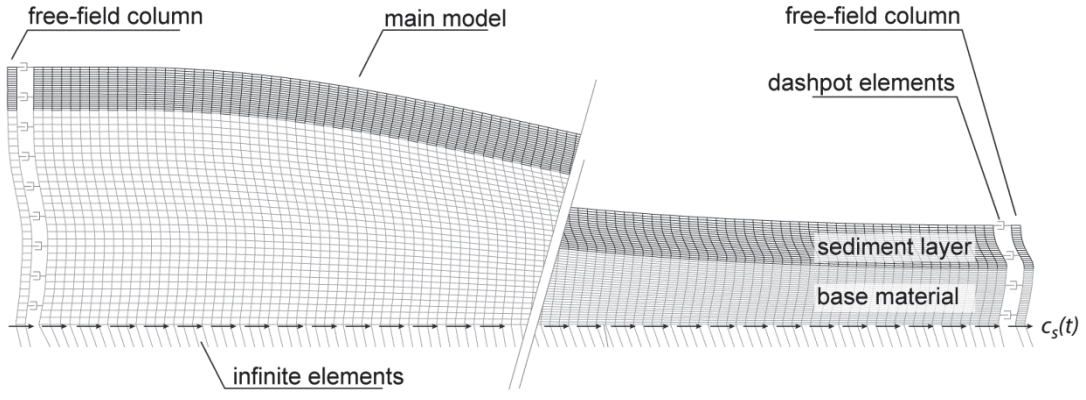

Fig. 2: Illustration of the finite element model for the seismic analysis

To avoid attenuation or reflection of waves at the lateral boundaries of the main model, the free-field boundary method is used (e.g. Nielsen 2014). The free-field columns on both sides of the main model correspond to horizontally layered ground with the same material properties as the main model at the respective boundary. Their movement is nearly unaffected by the main model but not the other way round (Nielsen 2014). To absorb outgoing waves from the main model, the free-field columns are coupled to the main model using dashpot elements.

Material properties varying within the sediment deposit, such as the bulk density ρ, the small strain shear modulus G_0 and the peak undrained shear strength q_{fu} are derived from the sedimentation analysis and mapped to the dynamic FE model (Stoecklin et al. 2018). Furthermore, the initial static stress field is derived from the sedimentation analysis results and serves as initial condition for the dynamic analysis. As the seismic FE model is formulated in total stresses, the initial stress is computed as the sum of the effective stress and the porewater pressure.

2.2.2 Constitutive model

Undrained simple shear tests on normally consolidated marine clay samples typically show and increase in shear stress up to a peak value during shearing, followed by a decrease in shear resistance until a residual value is reached. The peak shear strength strongly depends on the consolidation shear stress, whereas the residual strength at large strains seems to be nearly unaffected by it (Pestana et al. 2000). The strongly non-linear stress-strain behaviour of clays during undrained cyclic loading results in strain level dependent damping and is therefore important to consider in a dynamic analysis. One possible way of capturing this nonlinear hysteretic stress-strain behaviour during irregular cyclic loading is by using multi-surface kinematic hardening models (e.g. Prévost 1977). For this study such a multi-yield-surface kinematic hardening model was implemented in the FE code ABAQUS using a user subroutine. The numerical implementation of such multilayer plasticity models is described in detail by Montáns (2001). The model response for an element subjected to simple shear loading is illustrated in figure 3 for three different consolidation shear stress ratios. The stress-strain response is governed by the number of activated yield surfaces. By specifying the hardening moduli for each yield surface, a piecewise approximation of the non-linear stress-strain behaviour can be achieved. As a result of the kinematic hardening, the model response follows Masing rules during pre-peak unloading-reloading cycles. Isotropic strain softening is included, once the last yield surface becomes active to capture post-peak strain softening. The size of the external yield surface – the failure surface – is calculated as a function of the consolidation effective stress according to the Modified Cam Clay model (Roscoe & Burland 1970). To account for the stress-induced anisotropy, the inner yield surfaces in the initial

configuration are translated around the consolidation stress point prior to undrained shearing (Fig. 3a) (Prevost, 1977).

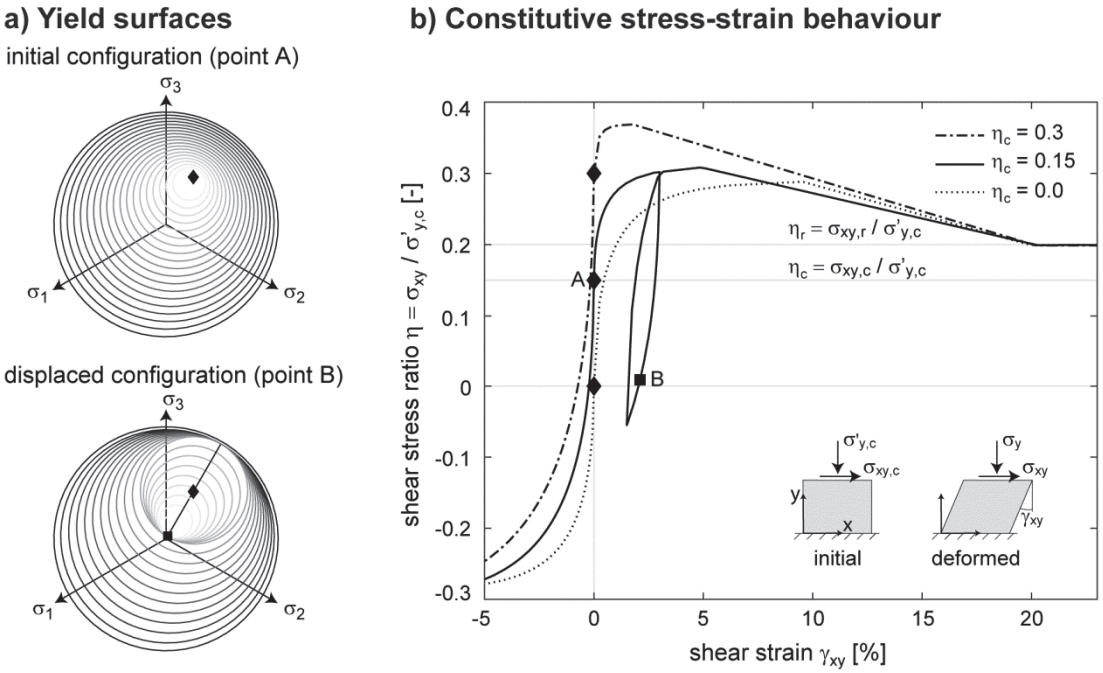

Fig. 3: Model response for an element subjected to simple shear loading starting from different initial consolidation shear stress ratios (η_c): (a) arrangement of the yield surfaces in the initial and the deformed configuration (corresponding to points A and B), (b) resulting stress-strain curves for three different consolidation stress ratios.

The strain-softening material behaviour can lead to a mesh dependency of the finite element solution. For this reason, a simplified scaling method is employed in this study, assuming that localized failure develops in a single element (e.g. Anastasopoulos et al. 2007). The post-peak softening branch of the stress-strain curve is scaled as a function of the element size.

3 Analysis of a 2D slope geometry

3.1 Geometry and initial conditions

Using the previously described methodology, two example cases are analysed. The slope geometry was chosen to follow a Gaussian curvature – a commonly observed morphology of submarine slopes (Adams & Schlager 2000) (Fig. 4a). To highlight the influence of the sediment deposition rate on the expected slope failure mechanism, two cases are analysed: in case A) the sediments are deposited at a very fast rate (e.g. over a relatively short time interval), whereas in case B) the

sediments are deposited over a 100-time longer time period. As a result, the slope in case B) is nearly normally consolidated, whereas in case A) the slope is significantly overpressured, resulting in a lower undrained shear strength and density in the lower part of the sediment deposit (Fig. 4b). In both cases the same mass of sediments is deposited on a stiff base, resulting in a sediment layer with a thickness of about $T \approx 23\ m$ and uniform intrinsic properties.

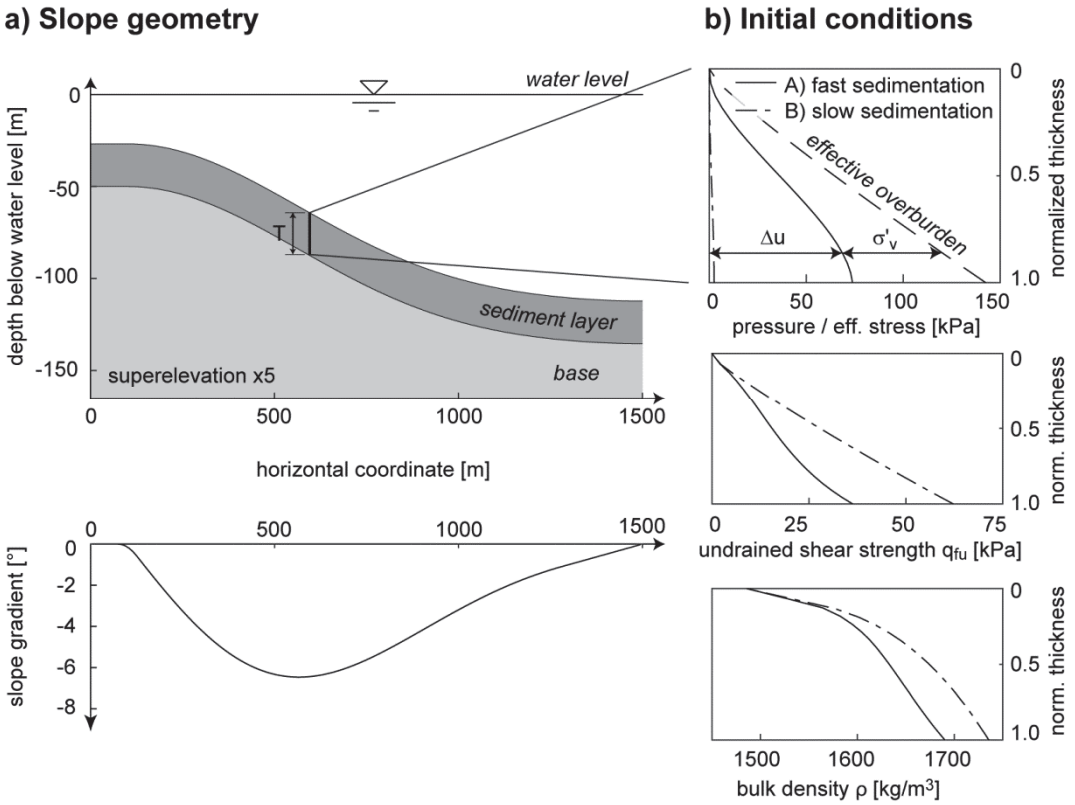

Fig. 4: (a) Slope geometry and curvature and (b) initial conditions for the dynamic analysis, shown in a cross section for both the overpressured (case A) and the normally consolidated slope (case B).

3.2 Results

For the example analysis, both the overpressured (case A) and the normally consolidated slope (case B) were subjected to the same ground motion record from the 1989 Loma Prieta earthquake (Fig. 5a). The time history has been retrieved from the PEER Strong Motion Database (PEER, 2013). Subjecting the overpressured slope to the earthquake input motion leads to a localization of shear strains at a particular depth and the nucleation of a narrow shear band. The evolution of shear strains during the seismic excitation shows that the shear band nucleates in the steepest part of the slope and grows progressively almost in parallel to the slope surface (Fig. 5b). After the earthquake, significant plastic strains have accumulated in the shear band, accompanied with a degradation of the

shear resistance, which makes the slope more susceptible to subsequent earthquake events. In case of the normally consolidated slope, on the other hand, the seismic excitation causes an accumulation of plastic strains near the seafloor, where the shear strength of the soil is lowest (Fig. 5c). Due to the pre-conditioning, the magnitude of the accumulated strains and strength degradation during the seismic loading is significantly larger in the overpressured slope compared to normally consolidated slope.

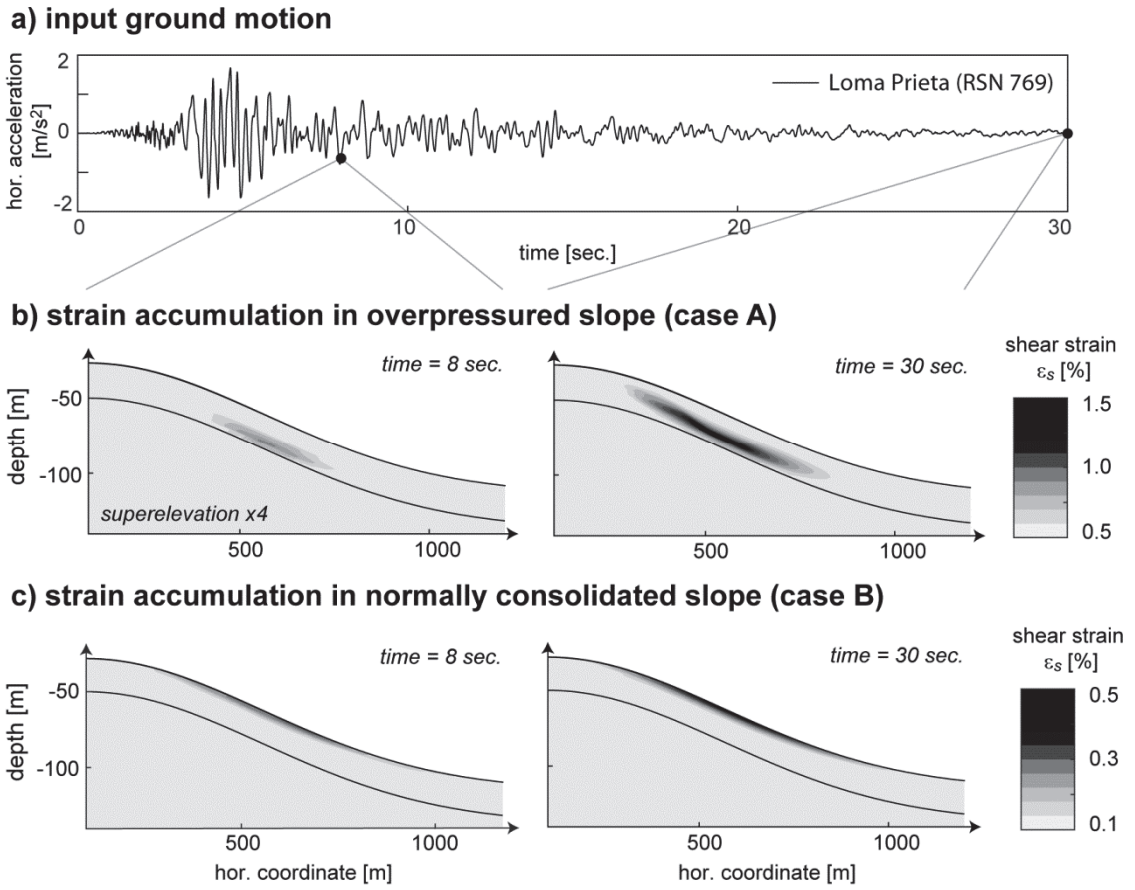

Fig. 5: Results from dynamic analysis: (a) applied input ground motion, (b) accumulated strains at different points during the seismic excitation in the overpressured slope and (c) in the normally consolidated slope profile (note the different scaling of the shear strain contours)

3.3 Discussion of the results

The results of the analysis show that subjecting the normally consolidated slope profile to the input ground motion leads to shearing of the sediments near the seafloor and the formation of a small slope failure mechanism near the seafloor. Similar results have been obtained in previous studies (e.g. Biscontin & Pestana 2006).

For the analysed overpressured slope, in contrast, shear strains accumulate in a localised shear band at a particular depth. This effect has also been observed in the

analysis of overpressured infinite slopes that were subjected to a wider range of input motions with different frequency spectra (Stoecklin et al. 2018). Once initiated, the shear band grows progressively during the seismic event. This process can continue until the shear band reaches the surface and a global slope failure mechanism is formed. If the shear band reaches a certain critical length before reaching the surface and the shear strength of the material has degraded sufficiently, the propagation can become self-driven, resulting in a catastrophic failure of the slope (Puzrin & Germanovich 2005). Using a simplified, quasi-static representation for earthquake loading, Stoecklin et al. (2017) showed that overpressures due to rapid sedimentation can set the conditions for such a slope parallel propagation of shear bands at a specific depth, along which slopes are prone to fail. The example analysis presented here illustrates how dynamic loading can initiate a localised failure zone in an overpressured sediment layer with homogeneous intrinsic properties at a particular depth and lead to progressive growth of the shear band. This mechanism can lead to large, slope-parallel mass movements – a morphological feature that has been observed in regions where sedimentation rates are high (McAdoo et al. 2000, ten Brink et al. 2016).

4 Conclusions

A two-step procedure is presented to simulate the seismic response of submarine slopes at different stages in the deposition process. In the first step, the sediment deposition is modelled, which provides the initial conditions for the subsequent second step – the seismic analysis. The procedure is outlined for plane-strain analyses, but could be applied for the analysis of 3D geometries as well by including free-field planes at the lateral boundaries in addition to the free-field columns. To capture the non-linear cyclic stress-strain behaviour of the deposited sediments, a multi-surface kinematic hardening model has been implemented. While the constitutive model allows accounting for strain-level dependent damping and post-peak strength degradation, it does not capture rate effects and degradation of pre-peak stiffness and peak strength during cyclic loading. These potential shortcomings remain to be refined in future studies.

The procedure is applied to analyse a 2D slope geometry. An overpressured and a normally consolidated slope profile were analysed as an example to highlight the effect of pre-conditioning on the expected slope failure mechanism. Subjecting the normally consolidated slope to seismic loading caused an accumulation of shear strains near the seafloor. In the overpressured slope, on the other hand, strains localized in a narrow shear band at a particular depth, leading to the initiation and progressive growth of an almost slope-parallel shear band, along which the slope is prone to fail. This would eventually result in a widespread mass movement with a much larger release volume.

The presented results are limited to the analysis of two extreme cases of very slow and very fast sedimentation rates. Considering a wider range of conditions and geometries could help identifying regions where pre-conditioning by sedimentation could lead to the emergence of large, potentially devastating mass movements and improve their hazard assessment.

5 Literature

Adams, E. W., & Schlager, W. (2000)
Basic Types of Submarine Slope Curvature. Journal of Sedimentary Research, 70(4), 814–828.

Anastasopoulos, I., Gazetas, G., Bransby, M. F., Davies, M. C. R., & El Nahas, A. (2007)
Fault Rupture Propagation through Sand: Finite-Element Analysis and Validation through Centrifuge Experiments. Journal of Geotechnical and Geoenvironmental Engineering, 133(8), 943–958.

Biscontin, G., & Pestana, J. M. (2006)
Factors affecting seismic response of submarine slopes. Natural Hazards and Earth System Science, 6(1), 97–107.

Dassault Systèmes Simulia, Fallis A, Techniques D (2013)
ABAQUS documentation. Abaqus 6.12, Providence, Rhode Island, USA.

Dugan, B., & Sheahan, T. C. (2012)
Offshore sediment overpressures of passive margins: Mechanisms, measurement, and models. Reviews of Geophysics, 50(3), 271–276.

Masson, D. G., Harbitz, C. B., Wynn, R. B., Pedersen, G., & Løvholt, F. (2006)
Submarine landslides: processes, triggers and hazard prediction. Philosophical Transactions. Series A, Mathematical, Physical, and Engineering Sciences, 364(1845), 2009–39.

McAdoo, B. G., Pratson, L. F., & Orange, D. L. (2000)
Submarine landslide geomorphology, US continental slope. Marine Geology, 169(1–2), 103–136.

Mejia, L. H., & Dawson, E. M. (2006)
Earthquake deconvolution for FLAC. In Proceedings of the 4th International FLAC Symposium on Numerical Modeling in Geomechanics (pp. 1–9).

Montáns, F. J. (2001)
Implicit multilayer J2-plasticity using Prager's translation rule. International Journal for Numerical Methods in Engineering, 50(2), 347–375.

Nielsen, A. H. (2014)
Towards a complete framework for seismic analysis in Abaqus, 167, 3–12.

PEER (2013)
PEER Ground Motion Database. Shallow Crustal Earthquakes Act. Tecton. Regimes, NGA-West2. URL http://ngawest2.berkeley.edu

Pestana, J. M., Biscontin, G., Nadim, F., & Andersen, K. (2000)
Modeling cyclic behavior of lightly overconsolidated clays in simple shear. Soil Dynamics and Earthquake Engineering, 19, 501–519.

Prévost, J.-H. (1977)
Mathematical modelling of monotonic and cyclic undrained clay behaviour. International Journal for Numerical and Analytical Methods in Geomechanics, 1(2), 195–216.

Puzrin, A. M., & Germanovich, L. N. (2005)
The growth of shear bands in the catastrophic failure of soils. Proceedings of the Royal Society A: Mathematical, Physical and Engineering Sciences, 461(2056), 1199–1228.

Roscoe KH, Burland JB (1970)
On the generalized stress-strain behavior of "wet" clay. Journal of Terramechanics, 7(2): 107–108.

Stoecklin, A., Friedli, B., & Puzrin, A. M. (2017)
Sedimentation as a Control for Large Submarine Landslides: Mechanical Modeling and Analysis of the Santa Barbara Basin. Journal of Geophysical Research: Solid Earth, 122(11), 8645–8663.

Stoecklin, A., Friedli, B., & Puzrin, A. M. (2018)
Seismic Response of Overpressured Submarine Slopes. In 16th European Conference on Earthquake Engineering. Thessaloniki.

Tappin, D. R., Watts, P., & Grilli, S. T. (2008)
The Papua New Guinea tsunami of 17 July 1998: Anatomy of a catastrophic event. Natural Hazards and Earth System Sciences, 8(2), 243–266.

ten Brink, U. S., Andrews, B. D., & Miller, N. C. (2016)
Seismicity and sedimentation rate effects on submarine slope stability. Geology, 44(7), 563–566.

Urgeles, R., & Camerlenghi, A. (2013)
Submarine landslides of the Mediterranean Sea: Trigger mechanisms, dynamics, and frequency-magnitude distribution. Journal of Geophysical Research: Earth Surface, 118(4), 2600–2618.